Experimental Verification of Isotropic Radiation from a Coherent Dipole Source via Electric-Field-Driven *LC* Resonator Metamaterials

Paul-Henri Tichit,[1] Shah Nawaz Burokur,[1,2] Cheng-Wei Qiu,[3] and André de Lustrac[1,2]
[1]*IEF, CNRS, UMR 8622, University Paris-Sud, 91405 Orsay Cedex, France*
[2]*University Paris-Ouest, 92410 Ville d'Avray, France*
[3]*Department of Electrical and Computer Engineering, National University of Singapore, 4 Engineering Drive 3, Singapore 117576, Singapore*
(Received 2 May 2013; revised manuscript received 25 July 2013; published 24 September 2013)

It has long been conjectured that isotropic radiation by a simple coherent source is impossible due to changes in polarization. Though hypothetical, the isotropic source is usually taken as the reference for determining a radiator's gain and directivity. Here, we demonstrate both theoretically and experimentally that an isotropic radiator can be made of a simple and finite source surrounded by electric-field-driven *LC* resonator metamaterials designed by space manipulation. As a proof-of-concept demonstration, we show the first isotropic source with omnidirectional radiation from a dipole source (applicable to all distributed sources), which can open up several possibilities in axion electrodynamics, optical illusion, novel transformation-optic devices, wireless communication, and antenna engineering. Owing to the electric-field-driven *LC* resonator realization scheme, this principle can be readily applied to higher frequency regimes where magnetism is usually not present.

DOI: 10.1103/PhysRevLett.111.133901 PACS numbers: 42.70.Qs, 41.20.Jb, 42.79.Ry

Although innovative electromagnetic notions continue to captivate minds [1–7], the antenna [8] has always been an indispensable source of light or radiation and important part of wireless communication systems that are widespread in laboratories and industries [9]. Brouwer's theorem [10] proves that a simple and finite source cannot have an isotropic radiation [11,12] pattern due to the obligation of polarization change for a simple and finite source. In his article, Brouwer demonstrated that no vector function can be continuous and tangent everywhere on the boundary of a sphere. As a consequence, there is a point ($r = R$, θ_0, ψ_0) on the sphere where all continuous vector functions have to be zero. Since the Poynting vector is defined by the vector product of the electric and magnetic fields, this prevents it from being perpendicular and constant everywhere on the boundary of a sphere and, therefore, isotropic emission. If isotropic radiation is obtained, the solution for Helmholtz's equation will have an infinitesimal point source of perfect symmetry in all directions. If not, then there will always be an extension in geometry breaking three-dimensional (3D) spherical symmetry regardless of the sources involved.

This problem occurs to all sources in electromagnetics and optics, as long as Maxwell's equations are valid. Hence, the significance of making an actual coherent dipole source to be isotropic certainly goes beyond antenna community, e.g., manipulation of axion electrodyanimcs [13], optical illusion [14], wireless communication [15], etc. We selected the microwave dipole source because it is more accessible in daily life and convenient to perform a proof-of-concept experiment.

The source can create photons from their charge acceleration. In this connection, almost all sources including antenna systems can be regarded equivalent to dynamic dipoles or multipoles which possess accelerated charges oscillating around the equilibrium. These dipoles, which are spatiotemporally coherent sources, emit photons of identical phase and amplitude. Therefore, perfect 3D spherically isotropic symmetry cannot be obtained unless a number of incoherent sources with sophisticated control of amplitudes, phases, and relative spacing are used [8]. Therefore, the isotropic radiation by an actual dipole source has not been validated hitherto (intrinsically prohibited in classic topology), though it has long been conjectured and used in characterization. Although engineering solutions have been found to design radio-frequency identification antennas producing nearly omnidirectional radiation [13,14], this again poses the fundamental scientific challenge and, thereby, significant value to this work achieving isotropic radiator for a simple coherent dipole source. As for achieving omnidirectional radiation of a single dipole, recently, a radially anisotropic zero-index metamaterial (RAZIM) shell has been proposed to generate perfect isotropic radiation in a two-dimensional space [15] by confining all 2-D anisotropic modes while keeping the isotropic mode propagating through [16]. It is, thus, still challenging to enhance the power yield for the antenna radiation due to the confinement of all anisotropic modes.

The solution to this problem may be found in transformation optics [4,5]. We experimentally demonstrate the isotropic radiation from an actual dipole source for the first time. Interestingly, this method, inspired by transformation optics, can enable the control of electromagnetic fields and engineering of new devices such as the

invisibility cloak [1,6,7,17–23], wormholes [24], waveguide connections [25–29], and antennas [30–36], by producing proper permittivity and permeability parameters. These devices can be realized by electric metamaterial fabrication, which are engineered by subwavelength artificial structures that produce necessary material properties corresponding to the space manipulation. We will employ space manipulation for making a dipole behave as an isotropic radiator and realize this equivalence by speculated nonmagnetic materials by electric-type metamaterials, which may pave the way for higher frequency scaling and realization of better isotropy.

In this Letter, we will focus on the creation of isotropic emission by a simple dipole inserted in a material calculated by transformation optics. It is more accessible to realize a metamaterial with weak inhomogeneity and anisotropy in 3-D cylindrical coordinates and to virtually compress the embedded dipole via radial component of cylindrical coordinates. We will further show the practical 2-D demonstration of an isotropic dipole at microwaves frequencies by judiciously engineering metamaterials to control the emission in a maximal solid angle with impedance matched between the metamaterial and the vacuum. To experimentally validate our isotropic emission, near-field distribution is measured which is in good agreement with theoretical simulation. Indeed, if one particularly selects an infinitely short source, it is much closer to the ideal point source, and, therefore, the radiation is approximately isotropic. The perfect isotropy is gradually degraded when the source becomes longer than a singular point. It is, thus, worthwhile mentioning that we demonstrated the isotropic performance for a half-wavelength dipole antenna, which is supposed to have a well-defined ∞-shape radiation pattern.

As depicted by the ray tracing for Poynting vectors in Fig. 1, a directive antenna in Fig. 1(a) (a current source with extended length) emitting along $\pm 90°$ directions is transformed to be emitting isotropically along all directions in Fig. 1(c), when an appropriately designed metamaterial surrounds the extended source. The photorealistic ray tracing in Fig. 1(b) reveals that a pin-hole camera (receiver) placed in the center will see a landscape where the zones in the vicinity of $-90°$ and $+90°$ directions are more clearly resolved. Once metamaterial corresponding to the space transformation delimited by the blue circle in Fig. 1(c) is introduced and placed around the directive source, the entire panorama is more evenly captured by the central camera as shown in Fig. 1(d).

The outermost region is maintained throughout the process. We exponentially stretch all the space enclosed by the outermost boundary such that the center area is expanded more in comparison to the parts near the outer boundary of the region (limited by the diameter D). Thus, any source placed in the center region will function equivalently as another virtual source of much reduced dimension. If the

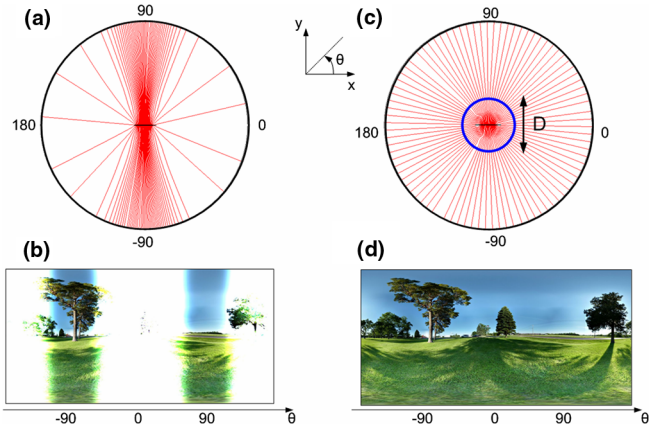

FIG. 1 (color online). A directive source emitting in the air as represented with the line of the Poynting vector (a) an equivalent receptor will see just two major part of a landscape. (b) An appropriate material is added in the central zone to create an isotropic radiation as represented with the Poynting vector (c). A receptor will see the entire landscape (d).

transformation is well manipulated, i.e., the expansion is complemented by the compression, perfect impedance matching at the boundary of the material can be achieved with no reflection.

Intuitively, the best transformation for isotropic radiation would have been to redistribute the angular component of the polar coordinates with a certain function $\theta' = g(r, \theta)$. The function g is able to make the source appear as a point by changing the direction of the light flow with an additional angular parameter in the transformation. Though it works with perfect theoretical permittivity and permeability parameters, the components are nondiagonal in polar coordinates. This transformation adversely results in metamaterials with stringently high values of permittivity and permeability which are difficult to realize, if not impossible. We have instead selected a radial transformation $r' = f(r, \theta)$ which leads to more plausible material parameters. It is noteworthy that this transformation optic method can approach near-perfect isotropy by significantly reducing the size of the physical dipole, though it may not be able to ideally reach the extreme equivalence of one point source considering the fabrication capability of metamaterials. The idea of the transformation is to reduce the size of the source such that it becomes a point source which is the only possible isotropic radiator. To do so, a space expansion is assured around the source, making its size appear very small with regard to the operating wavelength. This is then further covered by a compressed space in order to produce perfect impedance matching. Mathematically, the transformation has an exponential form and is given by [37]:

$$r' = \alpha(1 - e^{qr}), \qquad \theta' = \theta, \qquad z' = z, \tag{1}$$

with $\alpha = (D/2)(1/1 - e^{(qD/2)})$, where α is a function of the dimension of our material. Both α and q are constants.

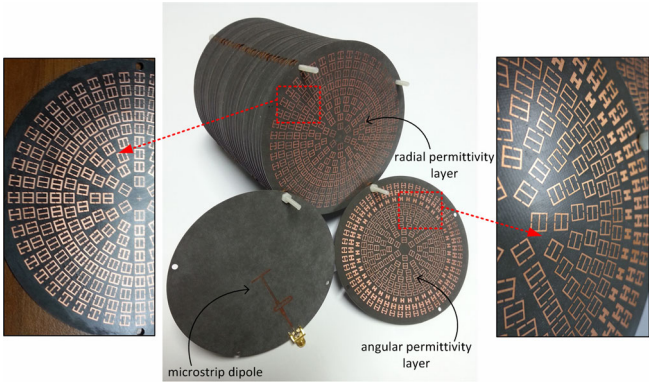

FIG. 2 (color online). Photography of the fabricated prototype consisting of alternating radial and angular electric permittivity metamaterial layers. In the experiment, a microstrip dipole antenna is used as the radiating source in the center of the stack.

Also, q must be negative for impedance matching and is the expansion factor of the stretched space. When q is high and close to zero, there is no change in the radiation pattern. On the contrary, a low q such as $q = -50$ leads to a nearly perfect isotropic radiation pattern. Interestingly, a full-parameter cloak has been suggested for one-directional invisibility [38] and it is challenging to design a full-parameter omnidirectional dipole hitherto. Therefore, the material derived from the rigorous transformation is still simplified due to fabrication constraints.

A dipole antenna operating at 10 GHz on a dielectric substrate (Fig. 2) is used as a radiating source along the y axis. Our surrounding material made of alternating layers of electric angular and radial metamaterial permittivity transforms the directive emission in the xy plane of the dipole into an isotropic one. Choosing a polarized electromagnetic field along the z direction fixes $\mu_{zz} = 1$, and we control $\varepsilon_{\theta\theta}$ and ε_{rr} only. The material is composed of nine different regions where radial and angular permittivities are not constant. We built the metamaterial from 30 layers of dielectric boards on which subwavelength resonant structures are printed. Fifteen layers contain artificial electric resonators [39] which assure radial permittivity. The remaining layers control angular permittivity. Each layer is divided into nine zones of metamaterial cells representing the inhomogeneous parameter distribution. The design geometries of these zones and their metamaterial cells has been provided in Supplemental Material [40]. The layers are stacked in an alternating manner, with a constant air spacing of 3.3 mm between neighboring layers. The overall dimensions of our antenna are $RH = 5$ cm $\times$ 12 cm, where R and H represent, respectively, the radius and the height of the antenna.

We present the metamaterial building blocks in Fig. 3(a) that meet the required parameters along radial and angular directions [shown in Fig. 3(c)]. The cell consists of two types of electric-field-driven LC resonators, as shown in Fig. 3(b). The metamaterial building block is not periodic, and two types of elementary resonators are optimized in one go since common parameters are shared. The distribution in Fig. 3(c) presents material parameters that we have discretized from an original continuous profile into nine regions of the metamaterial used for experimental validation. The imaginary parts (shown in the Supplemental Material [40] Fig. S3) of the material parameters are very low, suggesting negligible losses in the transformation medium.

The simulated cell is presented in Fig. 3(b). The permittivities ε_{rr} and $\varepsilon_{\theta\theta}$ can be achieved in a composite electric-field-driven LC resonator (ELC), thus providing electric responses that can be tailored. Taking the layout constraints under consideration, we chose a rectangular unit cell with dimensions $L_r = 5$ mm except for the first zone where we set $L_r = 20/3$ mm. We choose $L_\theta = (\pi/NL_r)[R_n^2 - R_{n-1}^2]$, where N represents the number of patterns in the nth zone and R_n is the radius of the nth zone. The desired ε_{rr} and $\varepsilon_{\theta\theta}$ were retrieved from S parameters by tuning geometric parameters of the resonators as

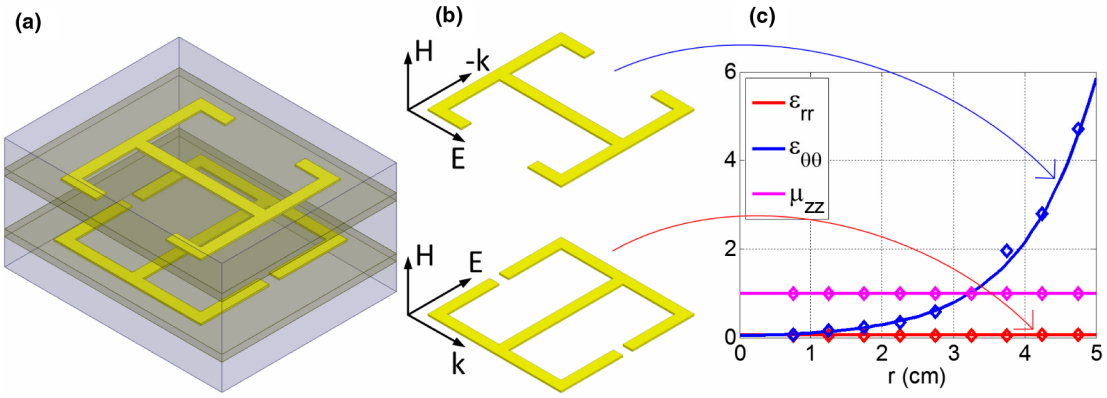

FIG. 3 (color online). (a) Metamaterial unit cell. (b) Each cell is composed of two electric-field-driven LC resonators enabling two varying parameters ε_{rr} and $\varepsilon_{\theta\theta}$. (c) The parameters from simplified transformation: theoretical values (continuous lines) and retrieved values based on the metamaterial cells (markers). It shows that $\varepsilon_{\theta\theta}$ ranges from 0.07 to 4.71 while ε_{rr} varies from 0.05 to 0.07.

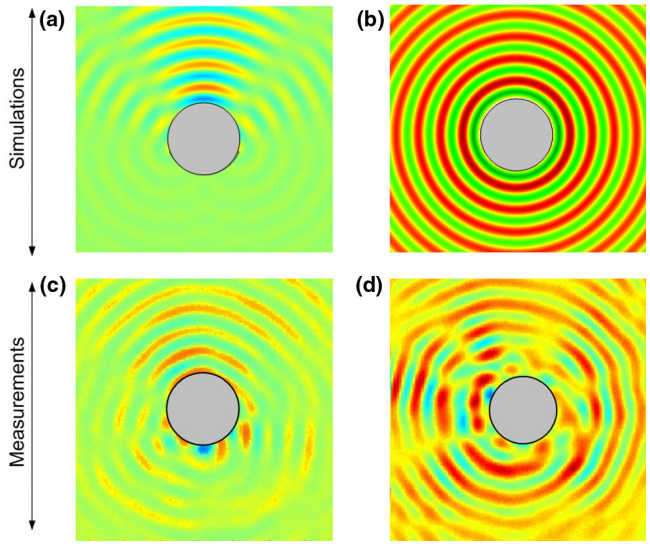

FIG. 4 (color online). Near-field scanning experiment in comparison with simulations. Magnitude of the electric field for the dipole source in simulation (a) and in measurement (c). Magnitude of the electric field of the dipole source and with the material defined with transformation optics in simulation (b) and in measurement (d). The mappings are shown at 10.8 GHz.

illustrated in Fig. 3(b). The discrete set of simulations and extractions are interpolated to obtain intermittent values of the geometric parameters that yield the material properties in Fig. 3(c). We observe that ε_{rr} takes on values close to zero. This is a consequence of setting q to -50 to achieve near-perfect isotropic emission in the xy plane. Impedance matching is assured in the proposed implementation. The operating frequency is selected set to approximately 10 GHz. This ensures $\lambda/L_r > 6$, where λ is the wavelength in free space. The design parameters of the unit cells and their retrieved parameters have been listed in the tables in Supplemental Material [40].

We present in Fig. 4(a) the theoretical result of the z component of electric field emanating from an ideal dipole antenna. When the dipole is surrounded with the metamaterial, the omnidirectional radiation can be obtained. This is presented in Fig. 4(b). The experimental verifications have been unambiguously demonstrated in Fig. 4(c) [measured radiation of Fig. 4(a)] and 4(d) [measured radiation of Fig. 4(b), respectively. An isotropic emission from an actual dipole antenna was thereby realized at originally a nonisotropic plane and measured by the near-field mapping of the antenna's radiation. It reveals that the directive radiation can be metamorphosed to be isotropic by the proposed metamaterials. The experimental setup was employed to probe the near field of the antenna's radiation. The E field is scanned by a field-sensing monopole probe connected to the network analyzer by a coaxial cable. The probe was mounted on two orthogonal linear translation stages (computer-controlled Newport MM4006), so that the probe could be translated with respect to the radiation region of the antenna. By stepping the field sensor in small increments and recording the field amplitude and phase at every step, a full 2-D spatial field map of the microwave near-field pattern can be acquired in the free-space radiation region. The total scanning area covers 400×400 mm^2 with a step resolution of 2 mm in lateral dimensions. Microwave absorbers are applied around the measurement stage in order to suppress undesired scattered radiations at the boundaries.

In this Letter, we have designed, fabricated, and demonstrated an almost isotropically emitting dipole source verified in the microwave regime, the principle of which is scalable in all frequencies of light especially for the currently used metmatateriall that does not rely on magnetic response. An anisotropic nonmagnetic metamaterial is realized by the ELC model, and its electric parameters are finely adjusted to meet the required material in the physical space which is manipulated by a particular radial transformation function to achieve omnidirectional emission in both xy and yz planes. Our result, verified by experimental measurements, paves the way for manipulating emission characteristics of various sources, fabricating nonmagnetic metamaterials for optical applications and enabling unprecedented applications in a wide spectrum of waves.

We thank Prof. Shuang Zhang in University of Birmingham for stimulating discussions and comments. We thank Eric Hendrix and Ahmed Mehmood for language editing, and grateful for the assistance from Alireza Akbarzadeh in Fig. 1. The authors acknowledge the support from French-UK project MIMICRA No. B0883 GEM1 ERG. C. W. Q. acknowledges the partial financial support from TDSI/11-004/1A from Temasek Defence Systems Institute.

[1] W. Cai, U. K. Chettiar, A. V. Kildishev, and V. M. Shalaev, Nat. Photonics **1**, 224 (2007).
[2] D. A. Genov, S. Zhang, and X. Zhang, Nat. Phys. **5**, 687 (2009).
[3] M. Rahm, S. A. Cummer, D. Schurig, J. B. Pendry, and D. R. Smith, Phys. Rev. Lett. **100**, 063903 (2008).
[4] U. Leonhardt, Science **312**, 1777 (2006).
[5] J. B. Pendry, D. Schurig, and D. R. Smith, Science **312**, 1780 (2006).
[6] D. Schurig, J. J. Mock, B. J. Justice, S. A. Cummer, J. B. Pendry, A. F. Starr, and D. R. Smith, Science **314**, 977 (2006).
[7] R. Liu, C. Ji, J. J. Mock, J. Y. Chin, T. J. Cui, and D. R. Smith, Science **323**, 366 (2009).
[8] C. A. Balanis, *Antenna Theory* (Wiley, New York, 1997).
[9] D. Roddy and J. Coolen, *Electronic Communications* (Prentice Hall, New York, 1999).
[10] L. E. J. Brouwer, KNAW Proc. **11**, 850 (1909).
[11] H. F. Mathis, Proc. IRE **39**, 970 (1951).
[12] W. K. Saunders, in *On the Unity Gain Antenna*, edited by E. C. Jordan, Electromagnetic Theory and Antennas (Macmillan, New York, 1963), Part 2, p. 1125.

[13] F. Wilczek, Phys. Rev. Lett. **58**, 1799 (1987).
[14] Y. Lai, J. Ng, H. Y. Chen, D. Z. Han, J. J. Xiao, Z.-Q. Zhang, and C. T. Chan, Phys. Rev. Lett. **102**, 253902 (2009); W. X. Jiang and T. J. Cui, Phys. Rev. E **83**, 026601 (2011).
[15] J. Soric, S. Maci, N. Engheta, and A. Alu, IEEE Trans. Antennas Propag. **61**, 33 (2013).
[16] Y. Kim, Microw. Opt. Technol. Lett. **55**, 375 (2013).
[17] S. L. Chen, K. H. Lin, and R. Mittra, Electron. Lett. **45**, 923 (2009).
[18] Q. Cheng, W. X. Jiang, and T. J. Cui, Phys. Rev. Lett. **108**, 213903 (2012).
[19] Y. Yuan, N. Wang, and J. H. Lim, Europhys. Lett. **100**, 34 005 (2012).
[20] W. Cai, U. K. Chettiar, A. V. Kildishev, V. M. Shalaev, and G. W. Milton, Appl. Phys. Lett. **91**, 111105 (2007).
[21] J. Li and J. B. Pendry, Phys. Rev. Lett. **101**, 203901 (2008).
[22] L. H. Gabrielli, J. Cardenas, C. B. Poitras, and M. Lipson, Nat. Photonics **3**, 461 (2009).
[23] U. Leonhardt and T. Tyc, Science **323**, 110 (2009).
[24] J. Valentine, J. Li, T. Zentgraf, G. Bartal, and X. Zhang, Nat. Mater. **8**, 568 (2009).
[25] T. Ergin, N. Stenger, P. Brenner, J. B. Pendry, and M. Wegener, Science **328**, 337 (2010).
[26] M. W. McCall, A. Favaro, P. Kinsler, and A. A. Boardman, J. Opt. **13**, 024003 (2011).
[27] A. Greenleaf, Y. Kurylev, M. Lassas, and G. Uhlmann, Phys. Rev. Lett. **99**, 183901 (2007).
[28] D. H. Kwon and D. H. Werner, New J. Phys. **10**, 115023 (2008).
[29] M. Rahm, D. A. Roberts, J. B. Pendry, and D. R. Smith, Opt. Express **16**, 11 555 (2008).
[30] D. A. Roberts, M. Rahm, J. B. Pendry, and D. R. Smith, Appl. Phys. Lett. **93**, 251111 (2008).
[31] J. Huangfu, S. Xi, F. Kong, J. Zhang, H. Chen, D. Wang, B.-I. Wu, L. Ran, and J. A. Kong, J. Appl. Phys. **104**, 014502 (2008).
[32] P. H. Tichit, S. N. Burokur, and A. de Lustrac, Opt. Express **18**, 767 (2010).
[33] U. Leonhardt and T. Tyc, New J. Phys. **10**, 115026 (2008).
[34] Y. Luo, J. Zhang, L. Ran, H. Chen, and J. A. Kong, IEEE Antennas Wireless Propagat. Lett. **7**, 509 (2008).
[35] F. Kong, B.-I. Wu, J. A. Kong, J. Huangfu, S. Xi, and H. Chen, Appl. Phys. Lett. **91**, 253509 (2007).
[36] P. H. Tichit, S. N. Burokur, D. Germain, and A. de Lustrac, Phys. Rev. B **83**, 155108 (2011).
[37] J. Allen, N. Kundtz, D. A. Roberts, S. A. Cummer, and D. R. Smith, Appl. Phys. Lett. **94**, 194101 (2009).
[38] C. Garcia-Meca, A. Martinez, and U. Leonhardt, Opt. Express **19**, 23 743 (2011).
[39] D.-H. Kwon, IEEE Antennas Wireless Propagat. Lett. **11**, 1125 (2012).
[40] See Supplemental Material at http://link.aps.org/supplemental/10.1103/PhysRevLett.111.133901 for detailed design of the ELC metamaterial cells and effective parameter extraction.